# A scaled mapping parabolic equation for sloping range-dependent environments

**Adam M. Metzler**[a)]
*Applied Research Laboratories, The University of Texas at Austin, 10000 Burnet Road, Austin, Texas 78758*
*ametzler@arlut.utexas.edu*

**Daniel Moran, Jon M. Collis, and P. A. Martin**
*Department of Applied Mathematics and Statistics, Colorado School of Mines, 1500 Illinois Street, Golden, Colorado 80401*
*daniel.jw.moran@gmail.com, jcollis@mines.edu, pamartin@mines.edu*

**William L. Siegmann**
*Department of Mathematical Sciences, Rensselaer Polytechnic Institute, 110 Eighth Street, Troy, New York 12180*
*siegmw@rpi.edu*

**Abstract:** Parabolic equation solutions use various techniques for approximating range-dependent interfaces. One is a mapping approach [M. D. Collins *et al.*, J. Acoust. Soc. Am. **107**, 1937–1942 (2000)] where at each range the domain is vertically translated so that sloping bathymetry becomes horizontal, and range dependence is transferred to the upper surface. In this paper, a scaled mapping is suggested where the domain is vertically distorted so that both the bathymetry and upper surface are horizontal. Accuracy is demonstrated for problems involving fluid sediments. Generalizations of the approach should be useful for environments with layer thicknesses that vary with range.


**PACS numbers:** 43.30.Dr, 43.20.Bi, 43.30.Es [GD]
**Date Received:** October 28, 2013 **Date Accepted:** January 16, 2014

## 1. Introduction

Parabolic equation solutions are efficient for range-dependent ocean wave propagation problems by marching solutions in range.[1] Accuracy in range-dependent environments is achieved by selecting an appropriate approach for treating sloping bathymetries and sediment interfaces. Current techniques include: Stair-step approximations,[2] where the domain is split into a series of range-independent regions and appropriate interface conditions are applied to march the solution between regions; coordinate rotations,[3] where the domain is effectively "rotated" such that the solution is marching parallel to the sloping bathymetry; and mapping approaches,[4] where the domain is mapped such that the bathymetry is flat. In this paper, a scaled mapping approach is introduced which maps the domain to one where both the bathymetry and upper surface are flat. This is in contrast to Ref. 4, where the domain is mapped translationally so that the bathymetry is flat and the range dependence is transferred to the surface. Examples are provided which demonstrate the accuracy of the approach for two ocean environments. The technique described in this paper should extend well to seismo-acoustic environments where current treatments of sloping bathymetries in parabolic equation (PE) approximations are not well handled.

[a)]Author to whom correspondence should be addressed.

 

## 2. Scaled mapping PE

For a time-harmonic source, the Helmholtz equation for a fluid with an axially symmetric coordinate system in the far-field ($rk \gg 1$) is[1]

$$\frac{\partial^2 p}{\partial r^2} + \rho \frac{\partial}{\partial z}\left(\frac{1}{\rho}\frac{\partial p}{\partial z}\right) + k^2 p = 0, \tag{1}$$

where $r$ and $z$ are range and depth, $p(r, z)$ is reduced complex pressure, $\rho(r, z)$ is density, and $k(r, z) = \omega/c(r, z)$ is acoustic wave number with angular frequency $\omega = 2\pi f$ and sound speed $c(r, z)$. Attenuation $\beta$, in units of dB/wavelength, is included by allowing the sound speed to be complex.[5] In this paper, the range dependence of the acoustic parameters is a result of a sloping bathymetric interface between the ocean and the sediment, modeled as an acoustic half-space, only. The range-dependent depth of the bathymetry is $b(r)$ and $h = \langle b(r) \rangle$ is the mean depth over all range. The surface $z = 0$ is assumed flat and satisfies a pressure-release condition.

To treat the bathymetric range dependence, a change of independent variables is applied:

$$\begin{pmatrix} \tilde{r} \\ \tilde{z} \end{pmatrix} = \begin{pmatrix} r \\ \gamma(r) z \end{pmatrix}, \tag{2}$$

where $\gamma(r) = h/b(r)$. This mapping transforms the original $(r, z)$ domain to a domain where both the bathymetric and surface interfaces are horizontal ($\tilde{z}|_{z=b(r)} = h$, $\tilde{z}|_{z=0} = 0$ for all $r$). In the context of numerical grid generation, Eq. (2) is known as a shearing transformation [see Eq. (1) in Ref. 6].

Substitution of Eq. (2) into Eq. (1) results in

$$\frac{\partial^2 p}{\partial \tilde{r}^2} - 2\tilde{z}\frac{b'}{b}\frac{\partial^2 p}{\partial \tilde{r}\partial \tilde{z}} + \tilde{z}\left[2\left(\frac{b'}{b}\right)^2 - \frac{b''}{b}\right]\frac{\partial p}{\partial \tilde{z}} + \tilde{z}^2\left(\frac{b'}{b}\right)^2 \frac{\partial^2 p}{\partial \tilde{z}^2} + \gamma^2 \rho \frac{\partial}{\partial \tilde{z}}\left(\frac{1}{\rho}\frac{\partial p}{\partial \tilde{z}}\right) + k^2 p = 0, \tag{3}$$

where $p = p(\tilde{r}, \tilde{z})$, $\rho = \rho(\tilde{z})$, $k = k(\tilde{z})$, and $b' = \mathrm{d}b/\mathrm{d}r = \mathrm{d}b/\mathrm{d}\tilde{r}$. Neglecting terms involving the slope $b'$ and curvature $b''$ reduces Eq. (3) to

$$\frac{\partial^2 p}{\partial \tilde{r}^2} + \gamma^2 \rho \frac{\partial}{\partial \tilde{z}}\left(\frac{1}{\rho}\frac{\partial p}{\partial \tilde{z}}\right) + k^2 p = 0, \tag{4}$$

which is the leading-order Helmholtz equation in the scaled domain. This assumption is equivalent to a small-slope approximation, and under this approximation the contributions of the ignored terms are negligible when compared to the remaining terns in Eq. (4). Equation (4) differs from Eq. (1) only by the $\gamma^2$ term in front of the $\tilde{z}$-derivative terms. Factoring Eq. (4) and retaining the outgoing operator yields the PE

$$\frac{\partial p}{\partial \tilde{r}} = ik_0\sqrt{1 + X}\,p, \tag{5}$$

where

$$X = \frac{1}{k_0^2}\left(\gamma^2 \rho \frac{\partial}{\partial \tilde{z}}\frac{1}{\rho}\frac{\partial}{\partial \tilde{z}} + k^2 - k_0^2\right), \tag{6}$$

and $k_0$ is a reference wave number. Equation (5) has a marching solution of the form

$$p(\tilde{r} + \Delta\tilde{r}) = \exp\left[ik_0 \Delta\tilde{r}\sqrt{1 + X}\right] p(\tilde{r}), \tag{7}$$

where $\Delta\tilde{r}$ is the range step, which can be numerically implemented by an appropriate approximation to the exponential of the square root operator. For this work, this will be achieved using a Padé approximation.[7]

Although the domain in the mapped coordinate system is range-independent in a geometric sense, with constant bathymetry and surface depths, the PE in Eq. (5) has range dependence on the operator $X$ through $\gamma(\tilde{r})$. Furthermore, the factorization used to obtain Eq. (5) is not exact because of the nonzero commutator term resulting from the dependence $\gamma(\tilde{r})$. The commutator term is

$$ik_0\left[(1+X)^{1/2}\frac{\partial p}{\partial\tilde{r}}-\frac{\partial}{\partial\tilde{r}}\left((1+X)^{1/2}p\right)\right]=-\frac{ik_0}{2}(1+X)^{-1/2}\left[2k_0^{-2}\gamma\frac{\mathrm{d}\gamma}{\mathrm{d}\tilde{r}}\rho\frac{\partial}{\partial\tilde{z}}\frac{1}{\rho}\frac{\partial}{\partial\tilde{z}}\right]p$$
$$\approx -ik_0^{-1}\gamma\frac{\mathrm{d}\gamma}{\mathrm{d}\tilde{r}}\rho\frac{\partial}{\partial\tilde{z}}\left(\frac{1}{\rho}\frac{\partial p}{\partial\tilde{z}}\right), \tag{8}$$

where a Taylor series approximation is used to simplify the term $(1+X)^{-1/2}$. Equation (8) represents an unaccounted contribution in Eq. (5). As expected, the left-hand side of Eq. (8) is zero if $X$ did not depend on $\tilde{r}$. To compensate for this term, a modified PE is used,

$$\frac{\partial p}{\partial\tilde{r}}=ik_0\sqrt{1+\hat{X}}p, \tag{9}$$

where

$$\hat{X}=\frac{1}{k_0^2}\left[\rho\left(\gamma^2-ik_0^{-1}\gamma\frac{\mathrm{d}\gamma}{\mathrm{d}\tilde{r}}\right)\frac{\partial}{\partial\tilde{z}}\frac{1}{\rho}\frac{\partial}{\partial\tilde{z}}+k^2-k_0^2\right]. \tag{10}$$

While $\hat{X}$ does not incorporate all effects of the commutator term in Eq. (8), it does account for a portion of them so that Eq. (9) provides potential improvement to Eq. (5).

The PE defined in Eq. (9) is also numerically implemented using a Padé approximation on the square root operator.[7] The operator $\hat{X}$ is approximated using finite differences in depth as defined in Ref. 8. The scale factor $\gamma(r)$ is discretized in range, so that $\hat{X}$ must be updated when $\gamma$ varies with range. Moreover, when $\hat{X}$ is updated both the scaled depth variable $\tilde{z}$ and step $\Delta\tilde{z}$ must also be updated. This implies that

$$\tilde{z}_j|_{\tilde{r}_1}\neq\tilde{z}_j|_{\tilde{r}_2}\quad\text{for}\quad\gamma(\tilde{r}_1)\neq\gamma(\tilde{r}_2), \tag{11}$$

where $\tilde{z}_j=j\Delta\tilde{z}$ is the $j$th discrete depth step in the mapped coordinates and $\tilde{r}_1$ and $\tilde{r}_2$ are two discrete ranges. Thus it is possible that for some $j$, $\tilde{z}_j$ may "cross" the bathymetric interface as the solution is marched in range, even though the bathymetry remains at a constant depth $h$ in the mapped domain. This case is handled by appropriately re-discretizing $k$ and $\rho$ at the appropriate discrete depths $\tilde{z}_j$, for $j=1,\ldots,N$ where $N$ is the maximum number of depth points, corresponding to the current range step. No interpolation is needed when re-discretization occurs as $\tilde{X}$ properly handles marching to the new discrete depths.

## 3. Examples

Solutions from the scaled mapping PE using Eq. (9) and translational mapping PE in Ref. 4 are compared, and the former is compared with reference solutions from the PE Range-dependent Acoustic Model (RAM).[9] Two example two-layer environments are examined to illustrate the accuracy of the scaled mapping PE. For both examples an artificial absorbing layer that prevents reflections lies below the acoustic sediment

Table 1. Acoustical parameters for examples A and B. Water parameters contain the subscript $w$, and bottom parameters contain the subscript $b$.

| Example | A | B |
|---|---|---|
| $c_w$ (m/s) | 1500 | See Eq. (13) |
| $\rho_w$ (g/ cm$^3$) | 1.0 | 1.0 |
| $\beta_w$ (dB/ $\lambda$) | 0.0 | 0.0 |
| $c_b$ (m/s) | 1704.5 | 1550 |
| $\rho_b$ (g/ cm$^3$) | 1.15 | 1.15 |
| $\beta_b$ (dB/ $\lambda$) | 0.5 | 0.5 |

layer, modeled as a fluid. Acoustical parameters for these examples are given in Table 1.

Example A examines a shallow-water environment containing a seamount. A 25 Hz point source is located 112 m in the ocean. The bathymetry is defined as:

$$b(r) = \begin{cases} 200, & r < 2400 \\ -2.8r + 6920, & 2400 < r < 2450 \\ 60, & 2450 < r < 2550 \\ 2.8r - 7080, & 2550 < r < 2600 \\ 200, & r > 2600, \end{cases} \tag{12}$$

where units of each term are meters. The seamount rises up 140 m from the seafloor and has a slope of approximately 70°, which is steep but not unreasonable for environments near continental shelves. Solutions are computed with $\Delta z = 1$ m and $\Delta r = 10$ m in the original domain. Transmission loss curves at receiver depth 30 m are depicted in Fig. 1 for the reference solution RAM (dashed line), the scaled mapping PE approach (solid line), and the translational mapping approach of Ref. 4 (dotted-dashed line), where the large-slope correction term described in Ref. 4 has been applied. The three curves are in agreement until the start of the seamount upslope at 2.4 km, after which the translational mapping solution differs strongly while the scaled mapping solution closely follows the reference solution. If the scaled mapping PE in Eq. (5) is used, the resulting solution matches the reference solution well in phase pattern; however, there are amplitude differences. These amplitude errors are not seen using Eq. (9), which is what is used for the scaled mapping PE in Fig. 1.

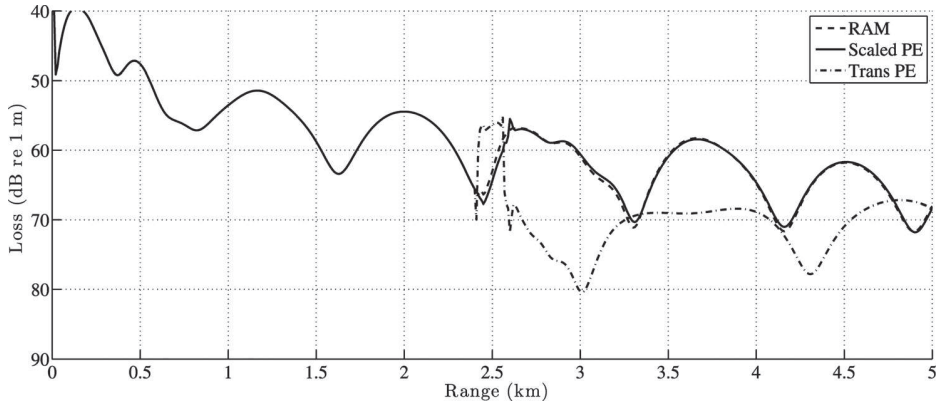


Fig. 1. Transmission loss curves for example A at receiver depth of 30 m using RAM (dashed line), the scaled mapping PE (solid line), and the translational mapping PE (dotted-dashed line).

The discrepancy of the translational mapping solution in Fig. 1 is a result of an inaccurate treatment of the bathymetry change. This is illustrated in Fig. 2 which shows transmission loss contours as functions of range and depth for example A. Figure 2(a) shows loss curves for the scaled mapping PE in the mapped domain $(\tilde{r}, \tilde{z})$. Both the bathymetry and surface interfaces are flat, with the bathymetry now located at $h = 195.81$ m. This solution mapped back into the original domain $(r, z)$ is shown in Fig. 2(b), where propagation through the seamount is clearly observed. Comparing Figs. 2(a) and 2(b) shows that the mapped domain is expanded near the seamount, when $h > b(r)$. Away from the seamount, the mapped domain is slightly contracted because $h < b(r)$; however, this is difficult to observe because $h$ is so close to $b(r)$. Figure 2(c) displays the result of the translational mapping PE solution after mapping back to the original domain. This method cannot handle the seamount, producing unphysical results in the water above the seamount and no transmission through the seamount. The reference solution using RAM is shown in Fig. 2(d) and is in excellent agreement throughout most of the domain with the scaled mapping solution in Fig. 2(b). The slight differences are attributed to the neglected terms in Eq. (3).

Example B is taken from the second example in Ref. 4 and examines propagation in a two-layer, deep-water, range-dependent environment with a depth-dependent sound speed. A 25 Hz point source is located 400 m into the ocean, which contains a depth-varying sound speed. The sound speed in the ocean is given by[10]

$$c_w(z) = c_*\left\{1 + \alpha\left[\frac{z - z_*}{H} + \exp\left(-\frac{z - z_*}{H}\right) - 1\right]\right\}, \tag{13}$$

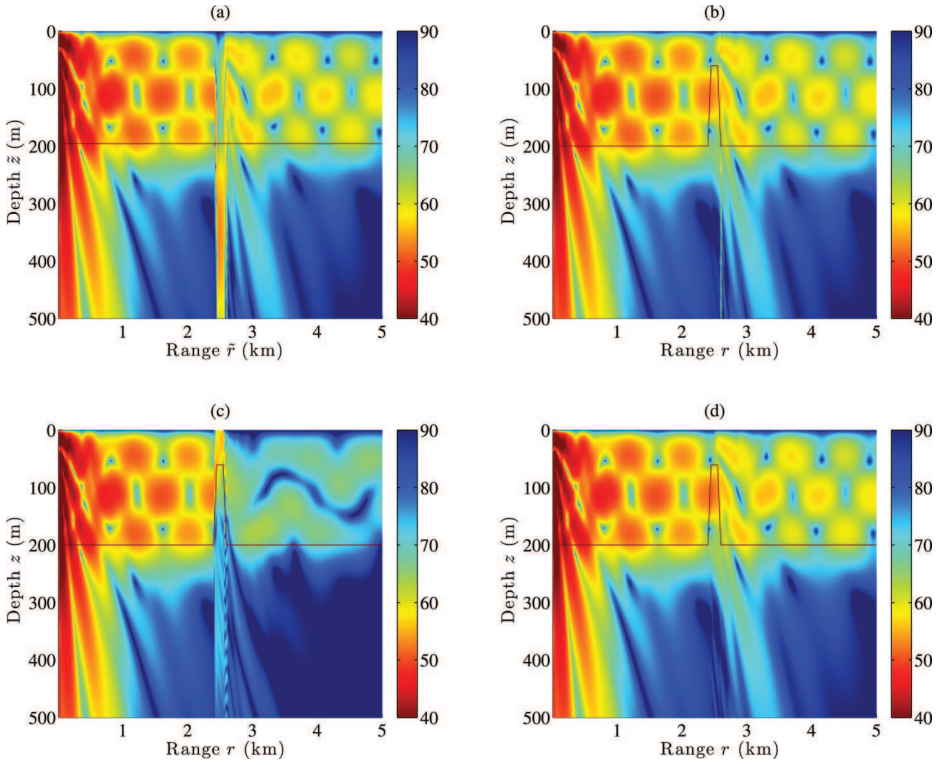


Fig. 2. (Color online) Transmission loss contours for example A. (a) The solution using the scaled mapping PE in the mapped domain. (b) The solution using the scaled mapping PE in the original domain. (c) The solution using the translational mapping PE in the original domain. (d) The solution using RAM.

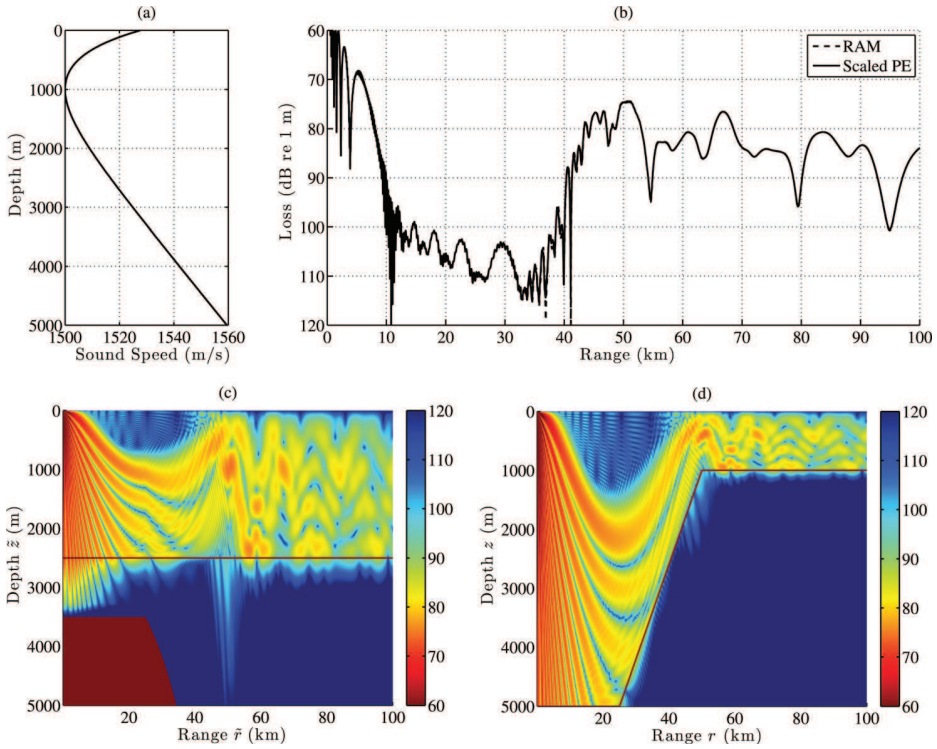


Fig. 3. (Color online) Results for example B. (a) Depth-dependent sound speed profile in the fluid. (b) Transmission loss curves at a receiver depth of 400 m for RAM (dashed line) and the scaled mapping PE (solid line). (c) The solution using the scaled mapping PE in the mapped domain. (d) The solution using the scaled mapping PE in the original domain.

where $c_* = 1500$ m/s, $H = 600$ m, $z_* = 1000$ m, and $\alpha = 0.007$, as shown in Fig. 3(a). The bathymetry is defined as

$$b(r) = \begin{cases} 5, & r < 25 \\ -0.16r + 9, & 25 < r < 50 \\ 1, & r > 50, \end{cases} \tag{14}$$

where all units are in kilometers. Solutions are computed with $\Delta z = 1$ m and $\Delta r = 10$ m in the original domain, and in the mapped domain $h = 2.5$ km. Transmission loss curves at a receiver depth of 400 m are given in Fig. 3(b) for the scaled mapping PE (solid line) and RAM (dashed line). The two curves are in excellent agreement for the 100 km propagation range. Loss contours for the scaled mapping PE solution are shown in the mapped domain in Fig. 3(c) and in the original domain in Fig. 3(d). Refractive beams due to the depth-dependent sound speed profile are seen in both contour plots. The solution in the mapped domain easily treats these beams by appropriately contracting and expanding the domain through the bathymetry changes in the original domain. The translational mapping solution (not shown) is in agreement with the curves in Fig. 3(b) and the contour in Fig. 3(d); as noted in Ref. 4, it requires a phase correction term to be applied to the solution. No such correction is required for the scaled mapping solution. Loss contours for Fig. 3(d) are in excellent agreement with those from RAM, as can be seen in Fig. 3 of Ref. 4.

## 4. Conclusions

A two-dimensional fluid PE is presented that treats range dependence through a scaled mapping technique. This approach maps the original domain, where the bathymetry varies with range, to one where both the bathymetry and surface are flat. Propagation in the mapped domain is obtained by appropriately expanding or contracting the waveguide as the solution is marched through range. The procedure is compared to reference solutions for shallow-water and deep-water environments and is shown to be more robust than a previous mapping approach, which distorts the waveguide only translationally. Future extensions are to incorporate the technique into seismo-acoustic PEs and to improve the solution by including some of the neglected terms in Eq. (3). Another extension is to environments with multiple layers or various thicknesses, requiring multiple scaled mappings to make all interfaces flat.

## Acknowledgments

The work of A.M.M. was supported by the Internal Research and Development program of the Applied Research Laboratories at The University of Texas at Austin. The work of W.L.S. was supported by the Office of Naval Research.

## References and links

[1]F. B. Jensen, W. A. Kuperman, M. B. Porter, and H. Schmidt, *Computational Ocean Acoustics* (AIP, New York, 1994), pp. 343–412.
[2]F. B. Jensen and W. A. Kuperman, "Sound propagation in a wedge-shaped ocean with a penetrable bottom," J. Acoust. Soc. Am. **67**, 1564–1566 (1980).
[3]M. D. Collins, "The rotated parabolic equation and sloping ocean bottoms," J. Acoust. Soc. Am. **87**, 1035–1037 (1990).
[4]M. D. Collins and D. K. Dacol, "A mapping approach for handling sloping interfaces," J. Acoust. Soc. Am. **107**, 1937–1942 (2000).
[5]F. B. Jensen, W. A. Kuperman, M. B. Porter, and H. Schmidt, *Computational Ocean Acoustics* (AIP, New York, 1994), pp. 35–37..
[6]P. R. Eiseman, "Grid generation for fluid mechanics computations," Ann. Rev. Fluid Mech. **17**, 487–522 (1985).
[7]M. D. Collins, "A split-step Padé solution for the parabolic equation method," J. Acoust. Soc. Am. **93**, 1736–1742 (1993).
[8]W. Jerzak, W. L. Siegmann, and M. D. Collins, "Modeling Rayleigh and Stoneley waves and other interface and boundary effects with the parabolic equation," J. Acoust. Soc. Am. **117**, 3497–3503 (2005).
[9]M. D. Collins, *User's Guide for RAM versions 1.0 and 1.0p, Technical report*, Naval Research Laboratory, Washington, DC (1995), pp. 1–14.
[10]W. H. Munk, "Sound channel in an exponentially stratified ocean with applications to SOFAR," J. Acoust. Soc. Am. **55**, 220–226 (1974).